Spectral decomposition and spectral balancing of seismic data

Satinder Chopra[1] and Kurt J. Marfurt[2]

Abstract

The interpretation of discrete stratigraphic features on seismic data is limited by its bandwidth and its signal-to-noise ratio. Unfortunately, well-resolved reflections from the top and base of subtle stratigraphic geologic boundaries occur only for thick features imaged by broadband data. Seismically thin stratigraphic features approaching a quarter-wavelength in thickness give rise to composite, or "tuned," seismic reflections. Different spectral-decomposition methods provide an effective way of examining the seismic response of stratigraphic geologic features in terms of spectral components and thus help in interpretation. Phase components help with interpretation of the discontinuity features as well as stratigraphic features such as onlap, offlap, and erosional unconformities. Applications of an often overlooked attribute derived during spectral decomposition, called the voice components, can be illustrated in terms of more accurate interpretation of the subsurface features. An "amplitude-friendly" method for spectral balancing enhances the frequency content of the data and preserves the geologic tuning features and amplitudes. Spectral decomposition of seismic data that are spectrally balanced and interpreted in terms of voice components leads to more accurate definition of the features of interest.

Introduction

Spectral decomposition of seismic data helps in the analysis of subtle stratigraphic plays and fractured reservoirs (Partyka et al., 1999; Marfurt and Kirlin, 2001). Given an input seismic trace in time, different spectral-decomposition methods — including the traditional short-window discrete Fourier transform, the continuous-wavelet transform (CWT), the S-transform, and the matching-pursuit transform — compute the spectral-magnitude and spectral-phase components at every time-frequency sample. The analysis of such spectral-magnitude and spectral-phase components is equivalent to interpreting subsurface stratigraphic features at different scales (Figure 1).

The mother wavelet chosen for CWT spectral decomposition, e.g., the Morlet wavelet, is a complex function (Sinha et al. 2005) (Figure 2). As a result, the spectral components obtained from CWT are also complex. Thus, when spectral decomposition is carried out on seismic data, it yields the spectral magnitude and phase at each time-frequency sample. The spectral magnitude represents the energy that correlates with the trace, and the phase represents the phase rotation between the seismic trace and the Morlet wavelet at each instant of time.

Goupillaud et al. (1984) show that the CWT process preserves the signal energy and is reversible. Thus the signal can be reconstructed from the CWT coefficients as a convolution along the scales used in the transformation plus an integration along time.

In addition to magnitude and phase, one can readily compute spectral voices (e.g., Marfurt and Matos, 2014) at every time-frequency sample. In this study, we discuss the value of such spectral voices in subsequent attribute calculation.

Another traditional use of time-varying Fourier transforms is spectral balancing. Trace-by-trace time-varying spectral balancing improves vertical resolution but destroys relative amplitudes. We discuss an "amplitude-friendly" method for flattening the amplitude spectra of the input data and show its applications as well.

Voice components from CWT spectral decomposition

In addition to spectral and phase components, Goupillaud et al. (1984) introduce another component, called the voice component, which is a simple function of spectral magnitude, m, and phase ϕ at each time-frequency sample and is given by

$$v(t,f) = m(t,f)\exp[-j\phi(t,f)]. \quad (1)$$

The real part of the sum over all frequencies, f, of all these voice components reconstructs the original trace. Because the voice

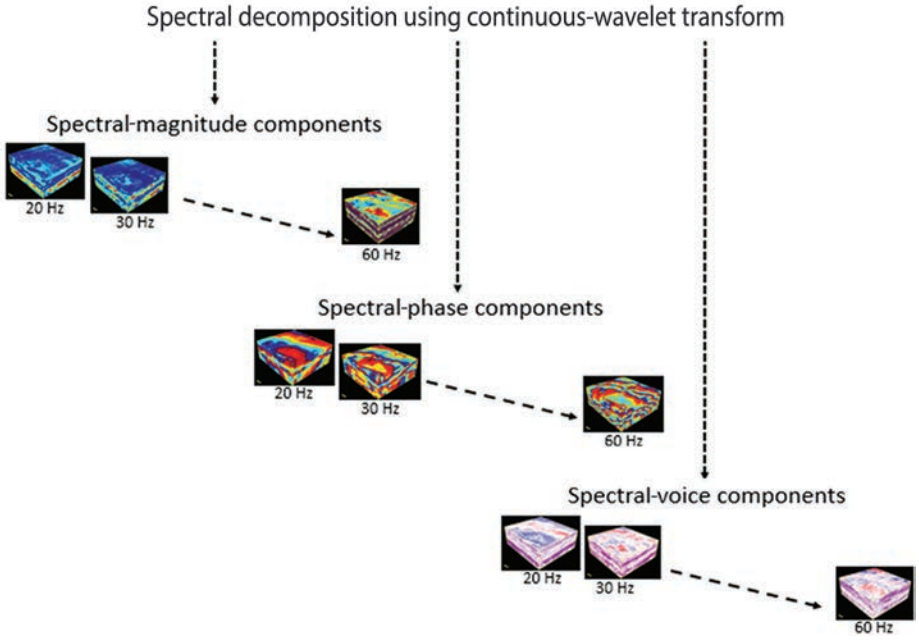

Figure 1. Typical workflow for spectral decomposition carried out by using the continuous-wavelet transform method. The output includes spectral-magnitude, spectral-phase, and spectral-voice component volumes.

[1]Arcis Seismic Solutions, TGS.
[2]University of Oklahoma.

http://dx.doi.org/10.1190/tle35020xxx.1.

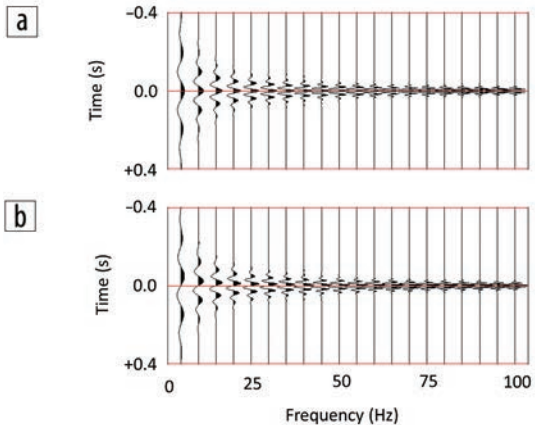

Figure 2. Complex wavelets used in the complex wavelet transform. The (a) real and (b) imaginary (or 90° phase-rotated) wavelets are simply convolved, with the input seismic trace about each sample to form v(t, f) and vH(t, f). The convolution with the real wavelets provides the voices, v(t, f), such as the 30-Hz voice shown in Figure 3. The spectral magnitude is defined as m(t, f) = {[v(t, f)]2 +]vH(t, f)]2}1/2, whereas the spectral phase is defined as ϕ(t, f) = ATAN2[vH(t, f),v(t, f)] and ranges between –180° and +180° (examples shown in Figure 4).

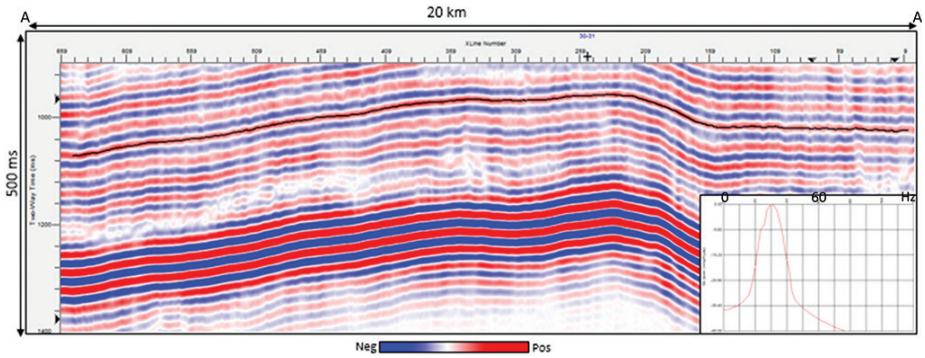

Figure 3. A vertical slice through the 30-Hz voice component after spectral decomposition with spectral balancing and its amplitude spectrum. Notice the frequency width on both sides of the amplitude maxima seen at 30 Hz. Data courtesy of Arcis Seismic Solutions, TGS.

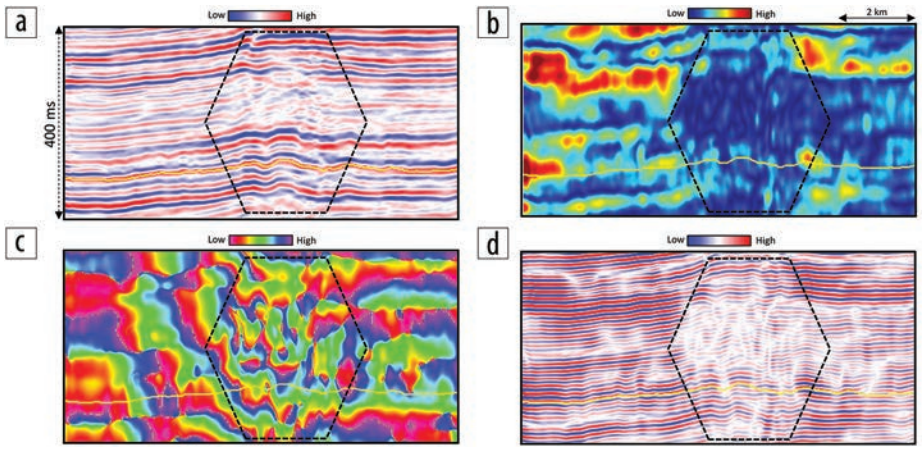

Figure 4. Vertical slices through (a) original 3D seismic amplitude and corresponding 65-Hz (b) spectral-magnitude, (c) spectral-phase, and (d) spectral-voice component volumes. Notice that vertical discontinuities in the highlighted portion are seen poorly in the original broadband data and are not seen in the spectral-magnitude component but are seen clearly in the spectral-phase and spectral-voice components. The voice component has the advantage that it can be interpreted and processed easily (e.g., using coherence), as the original seismic-amplitude data would. Data courtesy of Arcis Seismic Solutions, TGS.

components are band-pass-filtered versions of the original seismic data (Fahmy et al., 2008), the application to map subtle hydrocarbon features can be viewed as analysis of spectral voices.

After choosing an appropriate mother wavelet (Chopra and Marfurt, 2015), the scaled members of the wavelet family are defined by simple scaling and shifting of the mother wavelet. Crosscorrelating the member wavelets with the original seismic trace generates the spectral-voice components. For the continuous-wavelet transform, the voice components are equivalent to narrow bandpass-filtered versions of the input seismic data. We show the 30-Hz voice-component section in Figure 3, along with the magnitude spectrum of the 30-Hz wavelet.

Such voice components offer more information that subsequently can be processed and interpreted. In Figure 4a, we show a vertical slice through a 3D seismic volume from north-central Alberta, Canada. The equivalent slices through the spectral magnitude, phase, and voice components at 65 Hz are shown in Figures 4b, 4c, and 4d, which highlight fault discontinuities not seen in the original broadband data (or in most of the lower spectral components).

Notice that the vertical-discontinuity information is not seen clearly on the spectral magnitude but is clear on the phase component. The voice component combines both attributes and nicely delineates the discontinuities. This observation could be exploited to our advantage by interpreting the discontinuity information as such or by running discontinuity attributes such as coherence on the voice-component volume.

Since their introduction to the 3D interpretation community by Partyka et al. (1999), spectral-magnitude components have been used routinely to delineate stratigraphic features at or below the limits of seismic resolution. If a stratigraphic feature exhibits an approximately constant interval velocity, the tuning thickness is inversely proportional to the spectrally balanced peak frequency (e.g., Marfurt and Kirlin, 2001). More detailed information on seismic geomorphology can be gained by visualizing data at multiple frequencies, either through animation or by combining different spectral components using red-green-blue (RGB) color schemes (e.g., Li and Lu, 2014; Li et al., 2015).

Spectral balancing of seismic data in an amplitude-friendly way

The original short-window discrete Fourier-transform spectral decomposition introduced by Partyka et al. (1999) is good for analysis but cannot be used to reconstruct the original seismic data. By using a least-squares construct, Puryear and Castagna (2008) modified this algorithm to do so. The matching

pursuit, S-transform, and CWT also allow one to reconstruct the original seismic data.

Seismic processors have long known that if the input data are spectrally balanced or if their frequency bandwidth is extended somehow, the resulting volumes could lead to higher vertical and lateral resolution. We discuss an amplitude-friendly spectral-balancing method in this study, first discussed by Marfurt and Matos (2014).

In this method, data first are decomposed into time-frequency spectral components. The power of the spectral magnitude, $P(t,f) = m(t,f)^2$, is averaged over all the traces ($j = 1, \ldots K$) in the data volume spatially and in the given time window, which yields a smoothed average power spectrum, given by $P_{avg}(t,f)$. Next, the peak of the average power spectrum, $P_{peak}(t)$, also is computed.

Both the average spectral magnitude and the peak of the average power spectrum are used to design a single time-varying spectral-balancing operator that is applied to each and every trace in the data:

$$m_j^{bal}(t,f) = \left[\frac{P_{peak}(t)}{P_{avg}(t,f)+\varepsilon P_{peak}(t)}\right]^{\frac{1}{2}} m(t,f) \qquad (2)$$

where ε is the prewhitening parameter. A conservative value would be $\varepsilon = 0.04$. For larger surveys in which the estimate of the average spectra is statistically more robust, one might use values of $\varepsilon = 0.01$ in many cases, further broadening the spectrum. However, as with any filter, the interpreter needs to determine whether such aggressive spectral balancing introduces ringing in the data. Such spectral balancing is amplitude friendly because a single time-varying wavelet is applied to the entire data volume.

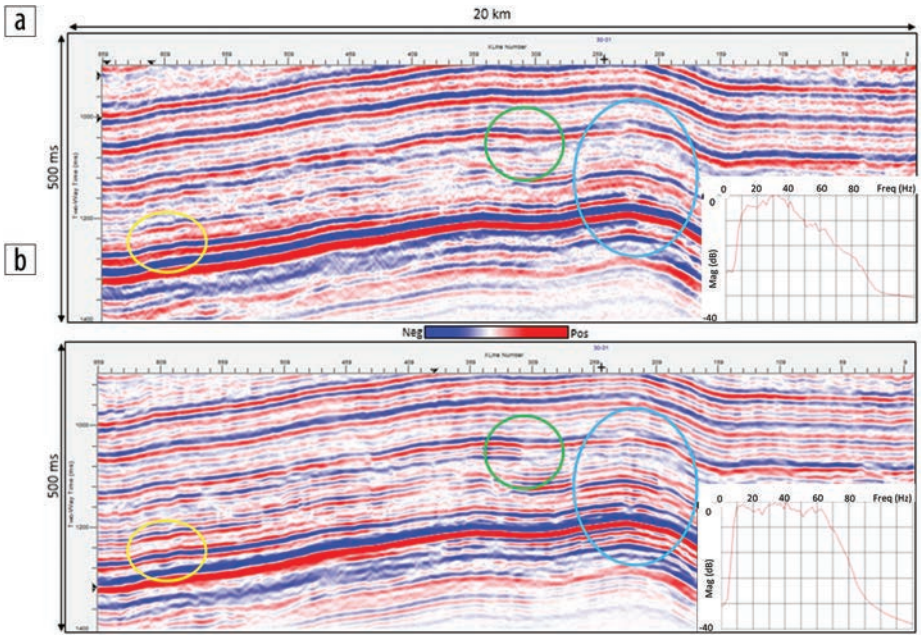

Figure 5. Vertical line through a seismic amplitude volume (a) before and (b) after spectral balancing. Note the small channel (yellow circle) and clear edge (green circle) and improved vertical resolution (cyan ellipse). Data courtesy of Arcis Seismic Solutions, TGS.

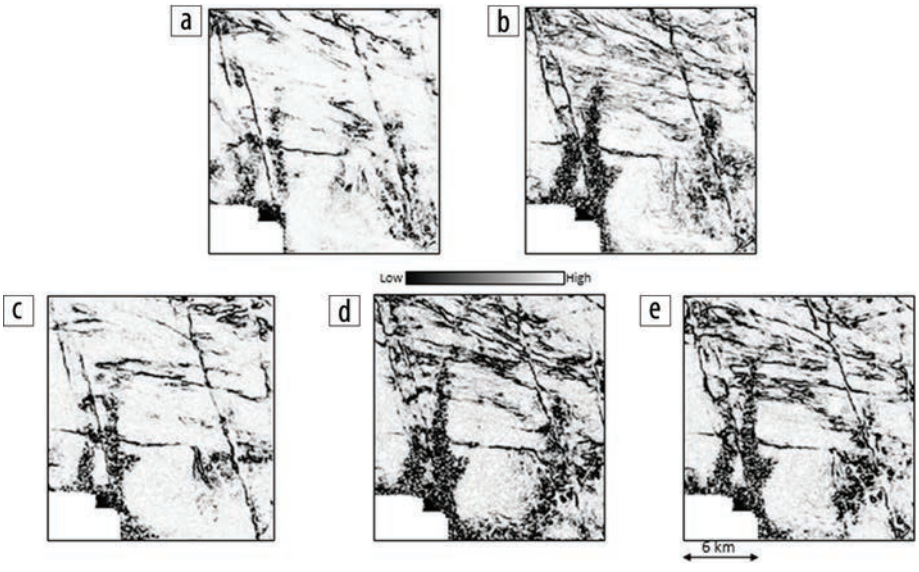

Figure 6. Time slices at 1322 ms (dotted line in Figure 4) through coherence computed from seismic data (a) before and (b) after spectral balancing and from the voice components at (c) 65 Hz, (d) 75 Hz, and (e) 85 Hz. Coherence computed from the voice components at 65, 75, and 85 Hz clearly shows the lineaments corresponding to faults and fractures. Data courtesy of Arcis Seismic Solutions, TGS.

Figure 5 shows vertical slices through a seismic-amplitude volume before and after spectral balancing. The spectra were computed at intervals of 5 Hz ranging from 5 to 120 Hz. The balancing was computed using a value of $\varepsilon = 0.04$. The individual amplitude spectra before and after are shown as insets.

Notice that after spectral balancing, the seismic section shows higher frequency content, and the amplitude spectrum is flattened. Encouraged with the higher-frequency content of the data, we run energy-ratio coherence (Chopra and Marfurt, 2008) on the input data as well as the spectrally balanced version of the data. The results are shown in Figures 6a and 6b, where we notice better definition of the north-northwest–south-southeast faults as well as the faults/fractures in the east-west direction on the coherence run on the spectrally balanced version.

Finally, we run spectral decomposition on the spectrally balanced version of the input seismic data and put the voice components through to energy-ratio coherence computation. In Figures 6c through 6e, we show equivalent time slices computed from the voice-component volumes of 65, 75, and 85 Hz. Notice the clarity in definition of the

discontinuities on the displays. Such data lead to better interpretation of discontinuities than carrying out the same exercise of the input data.

Conclusions

From the foregoing examples, we conclude two things: (1) Voice components derived from spectral decomposition of input seismic data furnish detailed and crisp information at specific frequencies that is amenable to more accurate interpretation. (2) Spectral balancing of seismic data, when performed in an amplitude-friendly way, leads to broader-band data, which exhibits detailed definition of faults and fractures. Such discontinuity information can be interpreted better on coherence displays in the zone of interest. Coherence-attribute computation performed on spectral voice components after spectral balancing yields higher detail with regard to faults and fractures or other discontinuity features such as channels, reefs, and so forth. TLE

Acknowledgments

We wish to thank Arcis Seismic Solutions, TGS, Calgary, Alberta, Canada, for encouraging this work and for permission to present these results.

Corresponding author: SChopra@arcis.com

References

Chopra, S., and Marfurt, K. J., 2008, Gleaning meaningful information from seismic attributes: First Break, **26**, no. 9, 43–53, http://dx.doi.org/10.3997/1365-2397.2008012.

Chopra, S., and K. J. Marfurt, 2015, Choice of mother wavelets in CWT spectral decomposition: 83rd Annual International Meeting, SEG, Expanded Abstracts, 2957–2961, http://dx.doi.org/10.1190/segam2015-5852193.1.

Fahmy, W. A., G. Matteucci, J. Parks, M. Matheney, and J. Zhang, 2008, Extending the limits of technology to explore below the DHI floor: Successful application of spectral decomposition to delineate DHIs previously unseen on seismic data: 78th Annual International Meeting, SEG, Expanded Abstracts, 408–412, http://dx.doi.org/10.1190/1.3054833.

Goupillaud, P., A. Grossman, and J. Morlet, 1984, Cycle-octave and related transforms in seismic signal analysis: Geoexploration, **23**, no. 1, 85–102, http://dx.doi.org/10.1016/0016-7142(84)90025-5.

Li, F., and W. Lu, 2014, Coherence attribute at different spectral scales: Interpretation, **2**, no. 1, SA99–SA106, http://dx.doi.org/10.1190/INT-2013-0089.1.

Li, F., J. Qi, and K. Marfurt, 2015, Attribute mapping of variable-thickness incised valley-fill systems: The Leading Edge, **34**, no. 1, 48–52, http://dx.doi.org/10.1190/tle34010048.1.

Marfurt, K., and M. Matos, 2014, Am I blue? Finding the right (spectral) balance: AAPG Explorer, http://www.aapg.org/publications/news/explorer/column/articleid/9522/am-i-blue-finding-the-right-spectral-balance, accessed 12 March 2015.

Marfurt, K. J., and R. L. Kirlin, 2001, Narrow-band spectral analysis and thin-bed tuning: Geophysics, **66**, no. 4, 1274–1283, http://dx.doi.org/10.1190/1.1487075.

Partyka, G., J. Gridley, and J. Lopez, 1999, Interpretational applications of spectral decomposition in reservoir characterization: The Leading Edge, **18**, no. 3, 353–360, http://dx.doi.org/10.1190/1.1438295.

Puryear, C. I., and J. P. Castagna, 2008, Layer-thickness determination and stratigraphic interpretation using spectral inversion: Theory and application: Geophysics, **73**, no. 2, R37–R48, http://dx.doi.org/10.1190/1.2838274.

Sinha, S., P. S. Routh, P. D. Anno, and J. P. Castagna, 2005, Spectral decomposition of seismic data with continuous-wavelet transform: Geophysics, **70**, no. 6, P19–P25, http://dx.doi.org/10.1190/1.2127113.